Application of Quadratically-Constrained Model Predictive Control in Power Systems

Tri Tran, Y. S. Foo. Eddy, and K-V. Ling
School of Electrical and Electronic Engineering,
Nanyang Technological University,
50 Nanyang Avenue, Singapore 639798.
Email: tcTran@ieee.org, eddyFoo@ntu.edu.sg,
ekvLing@ntu.edu.sg

Jan M. Maciejowski
Department of Engineering,
University of Cambridge,
Cambridge CB2 1PZ, United Kingdom.
Email: jmm@eng.cam.ac.uk

***Abstract*—Simulations for the *quadratically-constrained model predictive control* (QMPC) with power system linear models are studied in this work. In QMPC, the optimization is imposed with two additional constraints to achieve the closed-loop system stability and the recursive-feasibility simultaneously. Instead of engaging the traditional terminal constraint for MPC, both constraints in QMPC are imposed on the first control vector of the MPC control sequence. As a result, QMPC has the potential for further extension to the control of network centric power systems. The algorithm of QMPC has been developed in a previous paper. Here, simulation studies with small-signal linear models of three typical power systems are presented to demonstrate its efficacy. We also develop a computational strategy for the decentralized static state-feedback control using the same quadratic dissipativity constraint as of the QMPC. Only state constraints are considered in the state feedback design. A comparison is then provided in the simulation study of QMPC relatively to the constrained-state feedback control.**

I. Introduction

Decentralized control strategies are prevalent in the power system applications, see, e.g. [1], [2], [3], [4], and references therein. The developed QMPC is suitable to the decentralized control of interconnected systems rationalized by its engagement with the global information in the design phase. The *quadratic dissipativity constraint* [5] plays an important role in QMPC for assuring the closed-loop system stability. The linear matrix inequality (LMI) optimizations that compute the multiplier matrices for this constraint take the global information of the large-scale system into their formulations. As a result, the global interactions between subsystems are encapsulated by the dissipativity constraint. The deployment of such constraint for each individual QMPC in a decentralized architecture will, therefore, ensure the stability of the large-scale system. We have presented the QMPC algorithm developments for constrained linear systems in [6]. This paper emphasizes the application aspect of QMPC and focuses on the simulation studies with power systems.

The use of linearized models in load frequency control applications for power systems is justified by the small load variations in a nominal operating regime [7]. The treatment for nominal-linear plus nonlinear-coupling models such as those in the decentralized excitation control problems, e.g. [3], [4], [8], has also been presented elsewhere. QMPC algorithm for nonlinear input-affine systems is a subject of current research [9].

The small-signal linearized power system models used in this simulation study are: -

- A three-area power system with tie-lines for decentralized supplement load frequency control that includes a pre-designed local PI controllers, taken from [2];
- A four-area power system with tie-lines for decentralized power flow control, taken from [10]; and
- An isolated wind-diesel system supplement load frequency control, taken from [11]. The local PI controllers are also included in this example.

The reduced order nonlinear model of wind-diesel systems and the nominal-linear plus nonlinear-coupling models used in the decentralized excitation control problem can be referenced to, e.g., [12], [3], respectively. The QMPC strategy with the stability and recursive-feasibility constraints is firstly introduced in the sequel.

The optimization problem in QMPC is additionally imposed with two inequality constraints to achieve the closed-loop system stability and the recursive-feasibility. They are constraints on the first control vector of the MPC control sequence. The terminal constraint and the monotonically decreasing of Lyapunov function are not applicable to QMPC as usually are in the other traditional MPCs. As a direct result, the QMPC scheme is suitable for distributed and decentralized control of network systems and other forms of MPC such as multiplexed MPC [13] or economic MPC [14].

The quadratic dissipativity constraint plays an important role within the QMPC scheme. It is deployed as a stability constraint for assuring the closed-loop system stability. The quadratic dissipativity constraint resembles the generic dissipative property, defined by Jan C. Willems in [15], informally as $-\int_{t_0}^{T} s(t)dt \leq K$ for $T \geq t_0 \geq 0$. We engage the quadratic dissipativity constraint with the open-loop system

dissipativity [16] here to obtain the input-to-power-and-state stability (IpSS). IpSS is an extension of the input-to-state stability (ISS) [17], in which the power term $y^T w$ - inner product of the chosen output and input, is explicitly inclusive in the quadratic supply rate of the dissipation inequality. In parallel with the stability, the recursive feasibility is assured by the maximal one-step controllability criterion [18] in QMPC. It is also implemented by a constraint on the immediate future control vector. The assumption on the robustly constrained control invariant set [19] will guarantee that the constrained MPC problem has solutions.

This paper is organized as follows. Notations, existing results and the QMPC algorithm are outlined in Section 2. The stability condition is provided in this section. The decentralized constrained-state feedback is then developed in Section 3. Numerical simulations with small-signal linear models of three typical power systems demonstrate the effectiveness of QMPC in Section 4. Section 5 concludes this paper.

II. Preliminaries and QMPC Algorithm

A. Notation

Capital and lower case alphabet letters denote matrices and column vectors, respectively. $(.)^T$ denotes the transpose operation. $\|u\|_2$ is the ℓ_2-norm of vector u. $\|x\|_{\mathcal{Q}}$ is the weighted ℓ_2-norm of x, $\mathcal{Q} \succ 0$. $\|M\|_2$ is the induced 2-norm of matrix M. In the discrete time domain, the time index is denoted by k, $k \in \mathbb{Z}$. In symmetric block matrices, $*$ is used as an ellipsis for terms that are induced by symmetry. A function $\gamma : \mathbb{R}^+ \to \mathbb{R}^+$ belongs to class $\mathcal{K}$ if it is continuous, strictly increasing and $\gamma(0) = 0$. A function $\alpha : \mathbb{R}^+ \times \mathbb{R}^+ \to \mathbb{R}^+$ belongs to class $\mathcal{KL}$ if for each fixed $\ell \in \mathbb{R}^+$, $\alpha(.,\ell) \in \mathcal{K}$ and for each fixed $s \in \mathbb{R}^+$, $\alpha(s,.)$ is decreasing and $\lim_{\ell\to\infty} \alpha(s,\ell) = 0$.

B. System Model and Stability Condition

Consider an interconnected system Σ consisting of h subsystems, each denoted as $\mathscr{S}_i$, $i = 1, \ldots, h$ and has a discrete-time state equation of the form:

$$\mathscr{S}_i : \begin{cases} x_i(k+1) = A_i x_i(k) + B_i u_i(k) + E_i v_i(k) + L_i d_i(k), \\ w_i(k) = F_i x_i(k), \end{cases} \tag{1}$$

where $x_i(k) \in \mathbb{R}^{n_i}, v_i(k) \in \mathbb{R}^{m_{v_i}}$ and $w_i(k) \in \mathbb{R}^{q_{w_i}}$ are the state, interactive (or coupling) input and interactive output vectors respectively. $u_i(k) \in \mathbb{R}^{m_i}$ is the control input. (A_i, B_i) is controllable. d_i represents the unknown load disturbance, which is assumed a white noise sequence with zero mean and finite variances. But it is bounded by $\|d_i\|_2^2 \le \delta_i$. The constraints

$$\mathbb{U}_i := \{u_i : \ \|u_i\|_2^2 \le \eta_i, \ \eta_i > 0\}, \tag{2}$$

$$\mathbb{X}_i := \{x_i : \ \|x_i\|_2^2 \le \rho_i, \ \rho_i > 0\}, \tag{3}$$

$$\mathbb{V}_i := \{v_i : \ \|v_i\|_2^2 \le \theta_i, \ \theta_i > 0\}. \tag{4}$$

are considered herein. The interactive input $v_i(k)$ of subsystem $\mathscr{S}_i$ and the output $w_j(k)$ of subsystem $\mathscr{S}_j$, $i \neq j$, are connected to each other in an arbitrary topology. Using the definitions of block-diagonal matrices $A := \mathsf{diag}[A_i]_1^h$, the stacking vector $x := [x_1^T \ldots x_h^T]^T$, and similarly for the other matrices and vectors, the state equation of the large-scale system Σ is obtained in the following:

$$\Sigma : \begin{cases} x(k+1) = (A + EHF)x(k) + Bu(k) + Ld(k), \\ v(k) = Hw(k), \end{cases} \tag{5}$$

with a global coupling matrix H of entries 1 or 0 only.

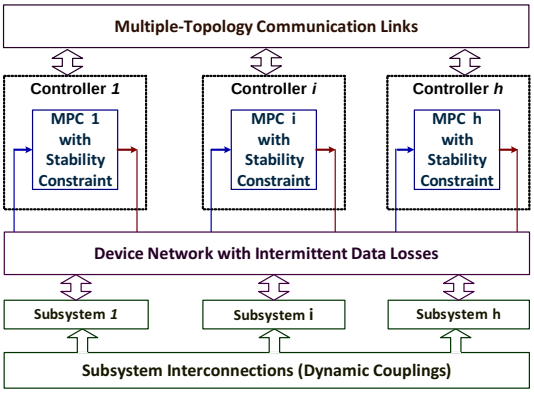

Fig. 1. The conceptualized block diagram of an interconnected system [5]. The top network (multiple-topology communication links) is not available in a decentralized control architecture. The intermittent data losses are not considered in this paper.

The conventional model predictive control (MPC) algorithm using $\mathscr{S}_i$ model (1) with $v_i \equiv 0$ in predictions will be deployed in this paper. We are concerned with the design of h decoupled stability constraints for these h local MPCs to achieve the overall control performance and the global stabilization.

The conceptualized block diagram of an interconnected system is given in Figure 1 with detailed captions. The stability constraint that has been derived from the quadratic dissipativity constraint in [6] is firstly provided in the next subsection.

C. Stability Constraint

Considering the quadratic supply rate $\xi(.,.)$ with respect to the input and state pair (u_i, x_i) for $\mathscr{S}_i$, the stability constraint for each subsystem is as follows:

$$u_i R_i u_i^T + 2x_i^T S_i^T u_i + \psi_i \le 0, \tag{6}$$

where $\psi_i(k) := x_i^T(k) Q_i x_i(k) - \beta_i \ \xi_i(k-1), \ 0 \le \beta_i < 1,$

in which $\xi(k-1)$ denotes the value of the supply rate $\xi(u_i, x_i)$ at the time step $k-1$. The constraint (6) will be imposed on the decentralized MPC optimization of each subsystem as an enforced stability constraint. (6) is convex if $R_i \succ 0$.

In QMPC, the closed-loop global system is input-to-power-and-state stable (IpSS). IpSS is an extension to ISS and defined as follows: Σ is *input-to-power-and-state stabilizable* (IpSS) if there are two functions α_1 and α_2 of class $\mathcal{KL}$, and there exists a function γ of class $\mathcal{K}$, such that for each bounded control u and disturbance d, each initial state $x_0 \in \mathbb{X}$ and

initial supply rate $\xi(u_{i(0)}, x_{i(0)})$, the solution exists for each $k \geq 0$, and furthermore, it satisfies

$$\|x(k)\|_2 \leq \alpha_1(\|x_0\|_2, k) + \alpha_2(|\xi_0|, k-1) + \gamma(\|d_{k-1}\|_2). \quad (7)$$

IpSS has been defined locally to ensure that the solution does practically exist. This is inferred from the fact that $V(x)$ (and thus $\|x(k)\|_2$) may diverge during certain time intervals when the term $\alpha_2(|\xi_0|, k-1)$ – a second $\mathcal{KL}$ function, is included in the inequality (7) of IpSS.

The next theorem states the sufficient stability condition for the interconnected system Σ. The LMI in this theorem is derived from the well known dissipation inequality [20].

Theorem 1: [6] Let $0 < \sigma < 1$. Denote $A_\Sigma := A + EHF$. Any controls $u_i(k),\ i = 1, 2, \ldots, h$, satisfying the stability constraint (6) that have the multiplier matrices $Q_i,\ S_i,\ R_i$ given by the following LMI optimization, for $x_0 = x(0)$:

$$\min_{P \succ 0, Q, S, R, \gamma} \quad x_0^T P x_0 \quad (8)$$

$$\text{s.t.} \quad \begin{bmatrix} P & PA_\Sigma & PB & PL \\ * & \sigma P + Q & S & 0 \\ * & * & R & 0 \\ * & * & * & (1-\gamma)I \end{bmatrix} \succcurlyeq 0,\ 0 < \gamma < 1,$$

for $Q := \mathsf{diag}[Q_i]_1^h,\ R := \mathsf{diag}[R_i]_1^h,\ S := \mathsf{diag}[S_i]_1^h$;

stabilize Σ in IpSS sense. □

The objective function $x_0^T P x_0$ is employed in (8) to maintain the global performance of $\sum_0^{+\infty} x_{(j)}^T P x_{(j)}$. For the recursive feasibility of the constrained state vector (3), the so-called feasibility constraint delineated in the next section will also be added to the MPC optimization.

D. Recursive Feasibility Constraint

The following inequality, called feasibility constraint, is considered in this paper:

$$u_i{}^T B_i^T B_i u_i + x_i^T A_i^T B_i u_i \leq \pi_i, \quad (9)$$

where $\pi_i := \frac{\rho_i}{3} - x_i^T A_i^T A_i x_i - \theta_i \|E_i^T E_i\|_2 - \delta_i \|L_i^T L_i\|_2$.

The feasibility constraint (9) has a solution when π_i is non-negative, for example, $u_i = 0$. For π_i being negative, a bound on the known state vector $x_i(k)$ is required. The following LMI-based condition renders the maximal 1-step controllable criterion [6]: $\operatorname{argmax}(\mu_i) \leq \pi_i$

$$\text{subject to} \quad \begin{bmatrix} B_i^T B_i + \lambda_i I_{m_i} & B_i^T A_i x_i \\ x_i^T A_i^T B_i & -\lambda_i \eta_i - \mu_i \end{bmatrix} \succcurlyeq 0,\ \lambda_i > 0.$$

For systems having control and state constraints, it is necessary to make some assumptions on the invariance of the constraint sets [19], in order for the problem to be feasible.

Definition 1: A set $\mathbb{X}_i \subset \mathbb{R}^{n_i}$ is called a robustly constrained control invariant with respect to $\mathbb{U}_i, \mathbb{V}_i$ and $\|d_i\|_2^2 \leq \delta_i$ of system $\mathscr{S}_i$ if for each $x_{i(k)} \in \mathbb{X}_i$, $\exists u_{i(k)} \in \mathbb{U}_i$, such that $x_{i(k+1)} \in \mathbb{X}_i$ for all $v_i \in \mathbb{V}_i$ and all bounded d_i, $\|d_i\|_2^2 \leq \delta_i$.

Assumption 1: $\mathbb{X}_i \subset \mathbb{R}^{n_i}$ is a robustly constrained control invariant set with respect to $\mathbb{U}_i$, $\mathbb{V}_i$ and $\|d_i\|_2^2 \leq \delta_i$ for the subsystem $\mathscr{S}_i$.

E. Quadratically-constrained MPC (QMPC)

The MPC computation procedure for each subsystem $\mathscr{S}_i$ is detailed in the following pseudo-algorithm:

Algorithm 1: QMPC for interconnected systems

1) The storage function matrix P and h sets of Q_i, S_i, R_i are computed off-line from the LMI optimization (8) in Theorem 1.
2) At every updating step k,
   a) Verify $\xi_{i(k-1)} \geq 0$ and $\psi_i < 0$. If *true*,
      i) The MPC optimization for the stand-alone $\mathscr{S}_i$ (1) with $v_i \equiv 0$, imposed with (6) and (9), is formed;
      ii) Otherwise, exclude the stability constraint (9) from the MPC optimization formulation.
   b) The MPC optimization is subsequently solved for the optimal control sequence $\hat{\mathbf{u}}_i^*(x_i)$. Only the first vector $u_i^*(0, x_i)$ of $\hat{\mathbf{u}}_i^*(x_i)$ is applied to control $\mathscr{S}_i$.
   c) Return to 2.a).

This algorithm only uses the multiplier matrices Q_i, S_i, R_i computed off-line, as in Step 1. The on-line updating algorithm for these Q_i, S_i, R_i matrices that help alleviate the conservativeness of (6) is presented in [6]. Both off-line and on-line updated multiplier matrices will be deployed for simulations in Section IV. To demonstrate the efficacy of QMPC, a static state feedback strategy is developed in the next section.

III. Decentralized Constrained-State Feedback

For the static state feedback strategy, the control constraint (2) is not considered in this development. The decentralized control law has the state feedback form of $u_i = K_i x_i$. The feedback gain K_i is used in the closed-loop derivations for the constraints (6), (9) and the dissipative condition (8) herein. It is necessary to consider the quadratic supply rate of

$$\xi(x_i, v_i) := v_i R_i v_i^T + 2 x_i^T S_i^T v_i + x_i^T Q_i x_i. \quad (10)$$

The quadratic dissipativity constraint is then

$$\xi(x_i(k+1), v_i(k+1)) \leq \beta_i \xi(x_i(k), v_i(k)),\ 0 \leq \beta_i < 1. \quad (11)$$

The following LMIs are derived from (11), (9), and the dissipation inequality for Σ of the form $x_+^T P x_+ - \sigma x P x \leq \sum_1^n \xi(x_i, v_i)$. They are obtained by substituting the model of Σ or $\mathscr{S}_i$ into the corresponding inequalities, rearranging them, and adequately applying the Schur complement:

$$\begin{bmatrix} \check{P} & K^T B^T + A_\Sigma^T & L^T \\ * & \sigma \check{P} + Y & 0 \\ * & * & (1-\gamma)I \end{bmatrix} \succcurlyeq 0, \quad (12)$$

$$\begin{bmatrix} 3\rho_i I & K_i^T B_i^T + A_i^T \\ * & (\rho_i - \nu_i) I \end{bmatrix} \succcurlyeq 0,\ i = 1, \ldots, n, \quad (13)$$

$$\begin{bmatrix} \check{M} & K^T B^T + A_\Sigma^T \\ * & \beta M \end{bmatrix} \succcurlyeq 0,\ P \succ 0,\ 0 < \gamma < 1, \quad (14)$$

where $M := Q + SHF + F^T H^T S^T + F^T H^T R H F$,

$K := \mathsf{diag}[K_i]_1^n,\ \beta := \min_i \beta_i,\ P := \mathsf{diag}[P_i]_1^n$,

$Q := \mathsf{diag}[Q_i]_1^n,\ S := \mathsf{diag}[S_i]_1^n,\ R := \mathsf{diag}[R_i]_1^n,$

$\nu_i := \theta_i \|E_i^T E_i\|_2 + \delta_i \|L_i^T L_i\|_2,\ M = PYP,\ \check{M} = M^{-1}.$

The computation for K_i is then as follows: Firstly, the matrices P, M and K are found from the solution to (12), (13), by the optimization of

$$\min_{P\succ 0, M\succ 0, K} \ x_0^T P x_0 \quad s.t.\ (12), (13). \tag{15}$$

Then assume $K_i^T = P_i^{-1} X_i^T$ and $M = ZP$. Thus, X_i, γ and Z are known with the resultant P from the above computation. Subsequently, P_i is re-computed by solving the equivalent LMIs of (12), (13), (14) for the minimum of γ with $0 < \gamma < 1$. The equivalent LMIs are provided below, for $X := \mathsf{diag}[X_i]_1^n$.

$$\begin{bmatrix} \check{P} & \check{P}X^T B^T + A_\Sigma^T & L^T \\ * & \sigma\check{P} + \check{P}Z & 0 \\ * & * & (1-\gamma)I \end{bmatrix} \succcurlyeq 0, \tag{16}$$

$$\begin{bmatrix} 3\rho_i I & \check{P}_i X_i^T B_i^T + A_i^T \\ * & (\rho_i - \nu_i) I \end{bmatrix} \succcurlyeq 0,\ i = 1, \ldots, n, \tag{17}$$

$$\begin{bmatrix} \check{P}Z^{-1} & \check{P}X^T B^T + A_\Sigma^T \\ * & \beta\check{P}Z \end{bmatrix} \succcurlyeq 0,\ \check{P} \succ 0,\ 0 < \gamma < 1. \tag{18}$$

And the LMI optimization of

$$\min_{P_i, \gamma} \ \gamma \quad s.t.\ (16), (17), (18), \tag{19}$$

will be solved for P_i and γ. The feedback gain computation is summarized below.

Algorithm 2: Static State-Feedback Gain Computation

1) Solve (15) for P, M and K.
2) Obtain $X_i = K_i P_i$ and $Z = MP^{-1}$.
3) Solve (19) for a new P.
4) Obtain $K_i = P_i^{-1} X^T$.

Simulations with small-signal power system models in Section IV will show the input and state trajectories from using $K_i = P_i^{-1} X_i$, as a result of Algorithm 2, and those from Algorithm 1 of QMPC.

IV. Numerical Simulations

Two multiple-area power systems with tie-lies and an isolated hybrid wind-diesel power system are studied in this section.

A. Supplement Load Frequency Control

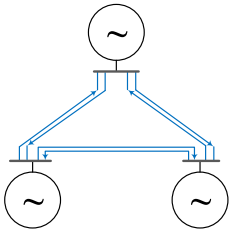

Fig. 2. A three-area power system with tie-lines for load frequency control.

The small-signal linearized model in this simulation study is of a three-area power system with tie-lines (see Figure 2) for decentralized load frequency supplement control that includes a pre-designed PI gains, borrowed from [2], [21], as follows:

$$A_i = \begin{bmatrix} -\frac{1}{T_{P_i}} & \frac{K_{P_i}}{T_{P_i}} & 0 & 0 & -\frac{K_{P_i}}{2\pi T_{P_i}} \sum_j K_{sij} \\ 0 & -\frac{1}{T_{T_i}} & -\frac{1}{T_{G_i}} & -\frac{1}{T_{G_i}} & 0 \\ -\frac{1}{R_i T_{G_i}} & 0 & -14.468 & -14.468 & 0 \\ K_{E_i} K_{B_i} & 0 & 0 & 0 & K_{E_i} \sum_j K_{sij} \\ 2\pi & 0 & 0 & 0 & 0 \end{bmatrix}$$

$$B_i = \begin{bmatrix} 0 \\ 0 \\ -\frac{1}{T_{G_i}} \\ 0 \\ 0 \end{bmatrix}, L_i = \begin{bmatrix} -\frac{K_{P_i}}{T_{P_i}} \\ 0 \\ 0 \\ 0 \\ 0 \end{bmatrix}, E_{i_{[j]}} = \begin{bmatrix} \frac{K_{P_i}}{2\pi T_{P_i}} K_{sij} \\ 0 \\ 0 \\ -\frac{K_{E_i}}{2\pi} K_{sij} \\ 0 \end{bmatrix}$$

The detailed model parameters from [2] are as follows:

$$A_1 = \begin{bmatrix} -0.05 & 6 & 0 & 0 & -0.955 \\ 0 & -3.472 & 3.472 & 0 & 0 \\ -5.878 & 0 & -13.021 & -13.021 & 0 \\ 4 & 0 & 0 & 0 & 1.592 \\ 6.283 & 0 & 0 & 0 & 0 \end{bmatrix},$$

$$B_1 = \begin{bmatrix} 0 \\ 0 \\ 13.021 \\ 0 \\ 0 \end{bmatrix}, L_1 = \begin{bmatrix} -6 \\ 0 \\ 0 \\ 0 \\ 0 \end{bmatrix}, F_1^T = \begin{bmatrix} 0 \\ 0 \\ 0 \\ 0 \\ 1 \end{bmatrix}, E_1 = \begin{bmatrix} .478 & .478 \\ 0 & 0 \\ 0 & 0 \\ -.796 & -.796 \\ 0 & 0 \end{bmatrix}$$

$$A_2 = \begin{bmatrix} -0.04 & 4.5 & 0 & 0 & -0.716 \\ 0 & -3.157 & 3.157 & 0 & 0 \\ -5.805 & 0 & -14.468 & -14.468 & 0 \\ 4 & 0 & 0 & 0 & 1.592 \\ 6.283 & 0 & 0 & 0 & 0 \end{bmatrix},$$

$$B_2 = \begin{bmatrix} 0 \\ 0 \\ 14.468 \\ 0 \\ 0 \end{bmatrix}, L_2 = \begin{bmatrix} -4.5 \\ 0 \\ 0 \\ 0 \\ 0 \end{bmatrix}, F_2^T = \begin{bmatrix} 0 \\ 0 \\ 0 \\ 0 \\ 1 \end{bmatrix}, E_2 = \begin{bmatrix} .358 & .358 \\ 0 & 0 \\ 0 & 0 \\ -.796 & -.796 \\ 0 & 0 \end{bmatrix}$$

$$A_3 = \begin{bmatrix} -0.05 & 5.75 & 0 & 0 & -0.915 \\ 0 & -2.976 & 2.976 & 0 & 0 \\ -6.448 & 0 & -14.881 & -14.881 & 0 \\ 4 & 0 & 0 & 0 & 1.592 \\ 6.283 & 0 & 0 & 0 & 0 \end{bmatrix},$$

$$B_3 = \begin{bmatrix} 0 \\ 0 \\ 14.881 \\ 0 \\ 0 \end{bmatrix}, L_3 = \begin{bmatrix} -5.75 \\ 0 \\ 0 \\ 0 \\ 0 \end{bmatrix}, F_3^T = \begin{bmatrix} 0 \\ 0 \\ 0 \\ 0 \\ 1 \end{bmatrix}, E_3 = \begin{bmatrix} .458 & .458 \\ 0 & 0 \\ 0 & 0 \\ -.796 & -.796 \\ 0 & 0 \end{bmatrix}$$

$$H = \begin{bmatrix} 0 & 1 & 0 \\ 0 & 0 & 1 \\ 1 & 0 & 0 \\ 0 & 0 & 1 \\ 1 & 0 & 0 \\ 0 & 1 & 0 \end{bmatrix}.$$

The block diagram of the ith area is shown in Figure 3.

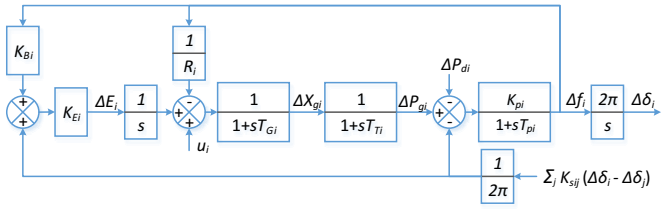

Fig. 3. Block diagram of the ith area control system [2].

The elements of the state vector $x_i = [\Delta f_i \;\; \Delta P_{g_i} \;\; \Delta X_{g_i} \;\; \Delta E_i \;\; \Delta\delta_i]^T$ are labeled along the signal lines in Figure 3. When the updating time is chosen at $\tau_s = 0.0225$ and the initial state vector is set up with $x(0) = 10^{-6} \times [6.3 \;\; 6.9 \;\; -8.4 \;\; -0.6 \;\; 1.2 \;\; 5.6 \;\; 8.8 \;\; -7.1 \;\; -1.2 \;\; 0.9 \;\; 12.2 \;\; 11.8 - 9.4 \;\; -0.2 \;\; 0.9]^T$, the computed state feedback gains are given below.

$$K_1 = \begin{bmatrix} -26.7724 \\ -31.1379 \\ -24.6646 \\ -44.8689 \end{bmatrix} \quad K_2 = \begin{bmatrix} 12.4068 \\ -1.5664 \\ 0.5280 \\ -249.5194 \end{bmatrix} \quad K_3 = \begin{bmatrix} 29.4551 \\ -1.1757 \\ -1.5268 \\ -499.5028 \end{bmatrix}$$

In this simulation, we have selected $\beta = 0.999$. The control and state trends are shown in Figures 4 and 5 for state feedback control and QMPC by Algorithm 1, respectively. The state response using the above decentralized state-feedback gains in Figure 4 shows a stabilized system. The decentralized QMPC is not only stabilized the system with a predictive horizon of 15 steps, but also improved the settling time and peaks. This can be seen clearly from the trends in Figure 5 relatively to Figure 4. It has been found in this example that the re-computation of multiplier matrices is not effective in this example.

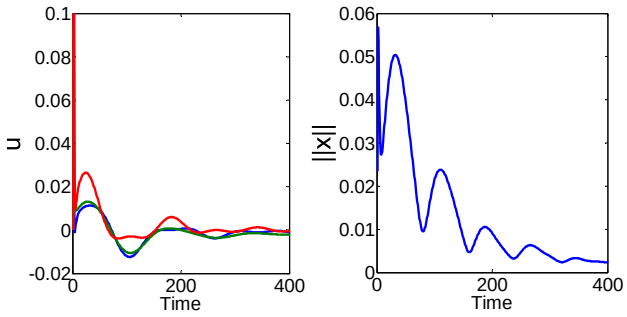

Fig. 4. Control and state trends from decentralized state feedback control.

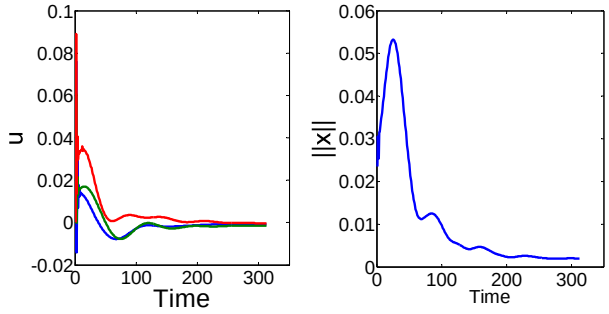

Fig. 5. Control and state trends from decentralized QMPC.

B. Power Flow Control

Figure 6 shows the block diagram of a four-area power system with tie-lines for the power flow control problem. This is also called automatic generation control (AGC) problem. The differential equations for an area is given below [10], [22].

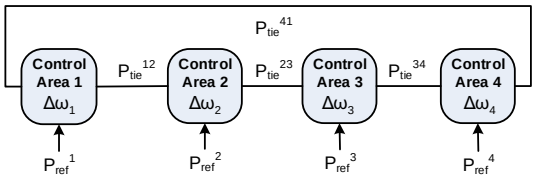

Fig. 6. A four-area power system with tie-lines for power flow control.

$$\begin{aligned}
\frac{d\Delta\omega_i}{dt} + \frac{1}{M_i^a} D_i \Delta\omega_i + \frac{1}{M_i^a} \Delta P_{\text{tie}^{ij}} - \frac{1}{M_i^a} \Delta P_{\text{mech}_i} &= -\frac{1}{M_i^a} \Delta P_{\text{L}_i}, \\
\frac{d\Delta P_{\text{mech}_i}}{dt} + \frac{1}{T_{\text{ch}_i}} \Delta P_{\text{mech}_i} - \frac{1}{T_{\text{ch}_i}} \Delta Z_{\text{v}_i} &= 0, \\
\frac{d\Delta Z_{\text{v}_i}}{dt} + \frac{1}{T_{\text{G}_i}} \Delta Z_{\text{v}_i} - \frac{1}{T_{\text{G}_i}} \Delta P_{\text{ref}_i} + \frac{1}{R_i^f T_{\text{G}_i}} \Delta\omega_i &= 0, \\
\frac{d\Delta P_{\text{tie}^{ij}}}{dt} &= T_{ij}(\Delta\omega_i - \Delta\omega_j), \\
\Delta P_{\text{tie}^{ij}} &= -\Delta P_{\text{tie}^{ij}}.
\end{aligned}$$

Nomenclature:

- ω : Angular frequency of rotating mass
- M^a : Angular momentum
- D : $\frac{\text{percentage change in load}}{\text{percentage change in frequency}}$
- P_{mech} : Mechanical power,
- P_{L} : Non-frequency sensitive load
- T_{ch} : Charging time constant of the prime mover
- Z_{v} : Steam valve position
- P_{ref} : Load reference set point
- R^f : $\frac{\text{percentage change in frequency}}{\text{percentage change in unit output}}$
- T_{G} : Governor time constant
- $P_{\text{tie}^{ij}}$: Tie-line power flow between areas i and j
- T_{ij} : Tie-line stiffness coefficient

Based on the model parameters from [10], we obtained the state realization matrices in the following:

$$A_1 = \begin{bmatrix} -0.75 & -0.25 & 0.25 & 0 \\ 2.19 & 0 & 0 & 0 \\ 0 & 0 & -0.02 & 0.02 \\ -0.833 & 0 & 0 & -0.25 \end{bmatrix},$$

$$B_1 = \begin{bmatrix} 0 \\ 0 \\ 0 \\ 0.025 \end{bmatrix}, F_1^T = \begin{bmatrix} 1 \\ 0 \\ 0 \\ 0 \end{bmatrix}, E_1 = \begin{bmatrix} 0 \\ -1.96 \\ 0 \\ 0 \end{bmatrix}$$

$$A_2 = \begin{bmatrix} -0.6875 & -0.25 & 0.25 & 0 \\ 2.54 & 0 & 0 & 0 \\ 0 & 0 & -0.1 & 0.1 \\ -0.5714 & 0 & 0 & -0.04 \end{bmatrix},$$

$$B_2 = \begin{bmatrix} 0 \\ 0 \\ 0 \\ 0.04 \end{bmatrix}, F_2^T = \begin{bmatrix} 1 \\ 0 \\ 0 \\ 0 \end{bmatrix}, E_2 = \begin{bmatrix} 0 \\ -2.45 \\ 0 \\ 0 \end{bmatrix}$$

$$A_3 = \begin{bmatrix} -0.275 & -0.1 & 0.1 & 0 \\ 1.8 & 0 & 0 & 0 \\ 0 & 0 & -0.1 & 0.1 \\ -0.667 & 0 & 0 & -0.02 \end{bmatrix},$$

$$B_3 = \begin{bmatrix} 0 \\ 0 \\ 0 \\ 0.02 \end{bmatrix}, F_3^T = \begin{bmatrix} 1 \\ 0 \\ 0 \\ 0 \end{bmatrix}, E_3 = \begin{bmatrix} 0 \\ -1.45 \\ 0 \\ 0 \end{bmatrix}$$

$$A_4 = \begin{bmatrix} -0.571 & -0.286 & 0.286 & 0 \\ 2.5 & 0 & 0 & 0 \\ 0 & 0 & -0.05 & 0.05 \\ -1.776 & 0 & 0 & -0.068 \end{bmatrix},$$

$$B_4 = \begin{bmatrix} 0 \\ 0 \\ 0 \\ 0.068 \end{bmatrix}, F_4^T = \begin{bmatrix} 1 \\ 0 \\ 0 \\ 0 \end{bmatrix}, E_4 = \begin{bmatrix} 0 \\ -2.46 \\ 0 \\ 0 \end{bmatrix}$$

$$H = \begin{bmatrix} 0 & 0 & 0 & 1 \\ 1 & 0 & 0 & 0 \\ 0 & 1 & 0 & 0 \\ 0 & 0 & 1 & 0 \end{bmatrix}.$$

The state vector of area ith consists of four elements, $x_i = [\Delta w_i \ \Delta P_{\text{tie}^{ij}} \ \Delta P_{\text{mech}_i} \ \Delta Z_{v_i}]^T$. When the updating time is chosen at $\tau_s = 0.1$, and the initial state vector is set up with $x_0 = 10^{-3} \times [4.5 \ 5.2 \ -6.8 \ -7 \ 4.6 \ 7.1 \ -8.2 \ -0.9 \ 10.2 \ 10.5 \ -10 \ -1 \ 10.2 \ 10.5 \ -10 \ -1]^T$, the computed feedback gains are as follows:

$$K_1 = \begin{bmatrix} -26.7724 \\ -31.1379 \\ -24.6646 \\ -44.8689 \end{bmatrix} \quad K_2 = \begin{bmatrix} 12.4068 \\ -1.5664 \\ 0.5280 \\ -249.5194 \end{bmatrix}$$

$$K_3 = \begin{bmatrix} 29.4551 \\ -1.1757 \\ -1.5268 \\ -499.5028 \end{bmatrix} \quad K_4 = \begin{bmatrix} 23.5298 \\ -0.4554 \\ 0.0524 \\ -146.5596 \end{bmatrix}.$$

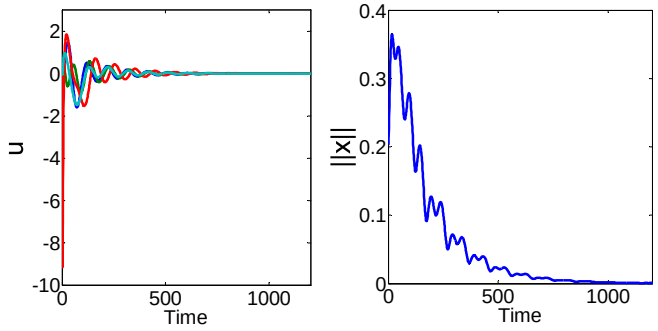

Fig. 7. Control and state trends from decentralized state feedback control.

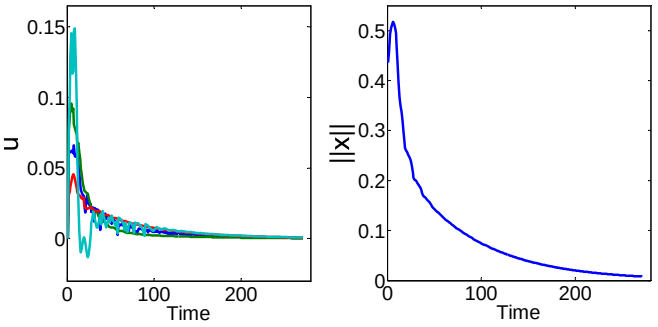

Fig. 8. Control and state trends from decentralized QMPC.

$\beta = 0.9999$ has also been selected in this simulation. Figure 7 shows the state and control trajectories using the above decentralized feedback gains. Similarly to first example above, the decentralized QMPC by Algorithm 1 is not only stabilized the system, but also improved the control performance in terms of settling time, compared to the state feedback control. The predictive horizon of $N_i = 6$ have been used for all four local MPCs in the simulations. The control constraints of $\eta_i = 0.4, \ i = 1, 2, 3, 4$ are imposed on respective subsystems. The weighting matrices of $\mathcal{Q}_1 = \text{diag}\{2, 1, 1, 1\}$, $\mathcal{Q}_2 = \text{diag}\{1, 1, 2, 1\}$, $\mathcal{Q}_3 = \text{diag}\{1, 2, 1, 1\}$, $\mathcal{Q}_4 = \text{diag}\{1, 1, 1, 2\}$, $\mathcal{R}_1 = \mathcal{R}_2 = \mathcal{R}_3 = \mathcal{R}_4 = = \text{diag}\{0.25\}$ are set up for the MPC cost functions.

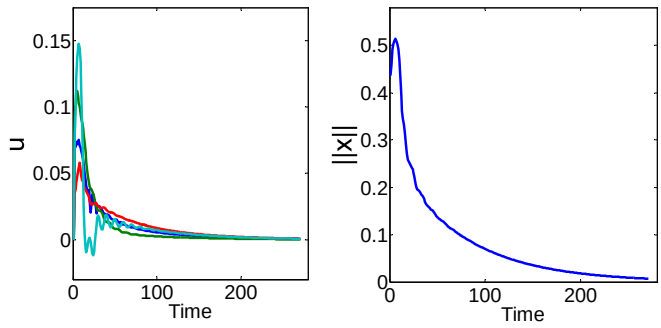

Fig. 9. Control and state trends from decentralized QMPC with re-computed multiplier matrices.

When the updating time is chosen at $\tau_s = 1.15$, and the initial state vector is selected as $x_0 = 10^{-2} \times [0.5 \ -2 \ 8 \ -1.7 \ 0.1 \ -1 \ -0.2 \ -1.9 \ 0.2 \ -1.5 \ 1 \ -1 \ 0.2 \ -0.5 \ 1 \ -1]^T$, the resulting control and state trends are depicted by Figures 8 and 9 for the QMPC with Algorithm 1, and the QMPC with dynamic multiplier matrices in [6], respectively. The control trajectories in Figure 9 are smoother than those in Figure 8, trading off for a much higher online computational cost.

C. Isolated hybrid power system

The small-signal linearized model of an isolated wind-diesel power system with local PI controllers, borrowed from [11], has been been used in this numerical example. Interested readers may refer to [12] for a nonlinear model of the isolated wind-diesel power system.

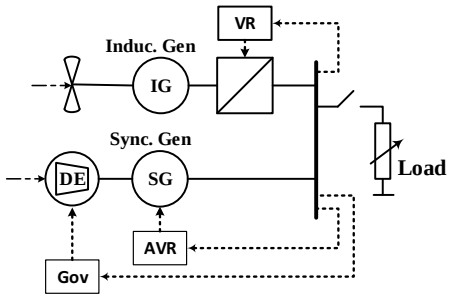

Fig. 10. Isolated wind-diesel power system.

This wind-diesel power system consists of a wind generator and a diesel generator connecting to a common bus bar. The wind generator has a wind turbine, an induction generator and the converter/inverter with its own voltage regulator. The diesel

generator has a diesel engine with governor and a synchronous generator with AVR (automatic voltage regulator), as sketched out by Figure 10.

Details of the control system transfer function block diagram is given in Figure 11. The supplement load frequency control here is to stabilize the system frequency and diesel generator power in the events of small load changes or wind power variations. The two states of interest are the deviations of system frequency and diesel power, which are the first and second elements in the state vector, respectively.

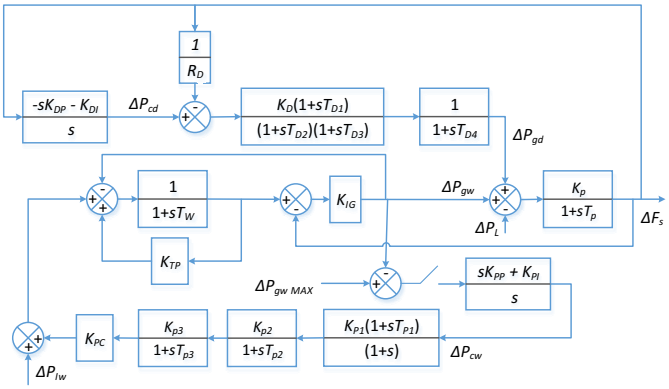

Fig. 11. Control system block diagram of an isolated wind-diesel power system [11].

$$A = \begin{bmatrix} -\frac{1+K_{IG}K_P}{T_P} & \frac{K_P}{T_P} & 0 & 0 \\ 0 & -\frac{1}{T_{D4}} & \frac{1}{T_{D4}} & \frac{1}{T_{D4}} \\ -\frac{K_D(T_{D2}-T_{D1})}{R_D T_{D2}(T_{D2}-T_{D3})} & 0 & -\frac{1}{T_{D2}} & 0 \\ -\frac{K_D(T_{D3}-T_{D1})}{R_D T_{D3}(T_{D3}-T_{D2})} & 0 & 0 & -\frac{1}{T_{D3}} \\ \frac{K_{IG}K_P}{T_W} & 0 & 0 & 0 \\ 0 & 0 & 0 & 0 \\ 0 & 0 & 0 & 0 \\ 0 & 0 & 0 & 0 \end{bmatrix}$$

$$\begin{bmatrix} \frac{K_{IG}K_P}{T_P} & 0 & 0 & 0 \\ 0 & 0 & 0 & 0 \\ 0 & 0 & 0 & 0 \\ 0 & 0 & 0 & 0 \\ -\frac{(1-K_{TP}+K_{IG})}{T_w} & \frac{1}{T_W} & 0 & 0 \\ 0 & -1 & \frac{K_{P3}K_{PC}K_{P1}}{T_{P3}} & \frac{K_{P3}K_{PC}K_{P1}T_{P1}}{T_{P3}} \\ 0 & 0 & -1 & 1-T_{P1} \\ 0 & 0 & 0 & -\frac{1}{T_{P2}} \end{bmatrix}$$

$$= \begin{bmatrix} -7.4 & 5 & 0 & 0 & 7.47 & 0 & 0 & 0 \\ 0 & -.333 & .333 & .333 & 0 & 0 & 0 & 0 \\ -.02 & 0 & -.5 & 0 & 0 & 0 & 0 & 0 \\ -1.58 & 0 & 0 & -40.0 & 0 & 0 & 0 & 0 \\ .374 & 0 & 0 & 0 & -.623 & .25 & 0 & 0 \\ 0 & 0 & 0 & 0 & 0 & -1 & .14 & .084 \\ 0 & 0 & 0 & 0 & 0 & 0 & -1 & .4 \\ 0 & 0 & 0 & 0 & 0 & 0 & 0 & -24.39 \end{bmatrix}$$

$$B = \begin{bmatrix} 0 & 0 \\ 0 & 0 \\ \frac{K_D(T_{D2}-T_{D1})}{T_{D2}(T_{D2}-T_{D3})} & 0 \\ \frac{K_D(T_{D3}-T_{D1})}{T_{D3}(T_{D3}-T_{D2})} & 0 \\ 0 & 0 \\ 0 & 0 \\ 0 & 0 \\ 0 & \frac{K_{P_2}}{T_{P_2}} \end{bmatrix} = \begin{bmatrix} 0 & 0 \\ 0 & 0 \\ .1013 & 0 \\ 7.8987 & 0 \\ 0 & 0 \\ 0 & 0 \\ 0 & 0 \\ 0 & 24.3903 \end{bmatrix} \quad L = \begin{bmatrix} 5 & 0 \\ 0 & 0 \\ 0 & 0 \\ 0 & 0 \\ 0 & .25 \\ 0 & 0 \\ 0 & 0 \\ 0 & 0 \end{bmatrix}$$

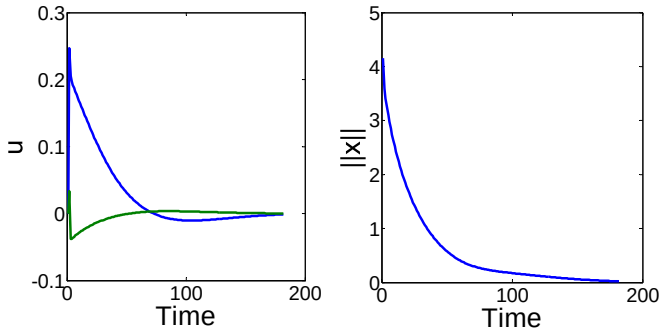

Fig. 12. Control and state trends from state feedback control.

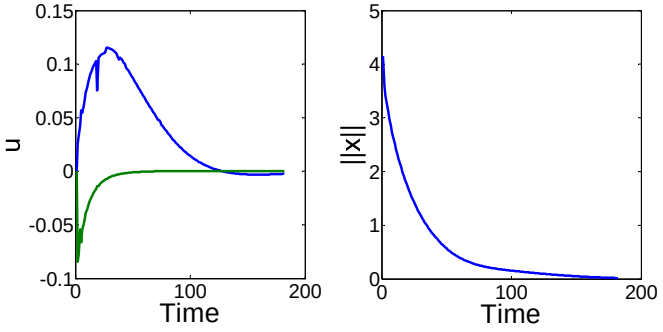

Fig. 13. Control and state trends from QMPC.

The updating time is chosen at $\tau_s = 0.1$. The initial state vector is set up with $x(0) = 10^{-2} \times [24.5\ \ 15.7\ \ -16.3\ \ -8.7\ \ 11\ \ -10\ \ 11\ -14]^T$. $\beta = 0.999$. The computed feedback gains are as follows:

$$K = -10^{-2} \times \begin{bmatrix} 141 & 91 & 101 & 104 & 138 & 138 & 118 & 511 \\ -792 & 74 & 206 & 422 & -245 & 59 & 326 & -18 \end{bmatrix}^T$$

The state response using the above state feedback gain in the control law shows a stabilized system. The QMPC by Algorithm 1 with a predictive horizon of $N = 6$ is not only stabilized the system, but also improved the control performance, in terms of settling time. The control and state trends are depicted by Figures 12 and 13 for state feedback control and QMPC, respectively. The control moves with QMPC are smaller and smoother than those with the state feedback.

The simulation studies in this section have demonstrated the effectiveness of QMPC, relatively to the static state-feedback control law, especially for decentralized control of power systems. The off-line computed multiplier matrices have also been found suitable for interconnected power systems, wherein the interactions between subsystems are quite moderate.

V. Conclusion

Simulation studies for QMPC using linearized models of two multiple-area power systems with tie-lines and of an isolated hybrid power system have demonstrated the suitability of QMPC for linear systems. Simulation studies for the non-linear input-affine model of wind-diesel power systems and

for the large-signal power systems having nominal-linear plus nonlinear-coupling models are presented elsewhere.

VI. Acknowledgement

The authors acknowledge the support by the Singapore National Research Foundation under its Campus for Research Excellence And Technological Enterprise (CREATE) programme.

References

[1] Khayyer, P. and U. Özgüner, "Decentralized control of smart grid with fixed and moving loads," *Proc. of IEEE Intl. Power and Energy Conference PECI'13*, pp. 72–75, Champaign, IL, USA, 2013.

[2] Mi, Y., Y. Fu, C. Wang, and P. Wang, "Decentralized sliding mode load frequency control for multi-area power systems," *IEEE Trans Power Systems*, vol. 28, no. 4, pp. 4301–4309, 2013.

[3] Zecevic, A. I., G. Neskovic, and D. D. Siljak, "Robust decentralized exciter control with linear feedback," *IEEE Trans Power Systems*, vol. 12, no. 6, pp. 1096–1103, 2004.

[4] Mahmud, M. A., H. R. Pota, M. Aldeen, and M. J. Hossain, "Partial feedback linearizing excitation controller for multimachine power systems to improve transient stability," *IEEE Trans Power Systems*, vol. 29, no. 2, pp. 561–571, 2014.

[5] Tri Tran and Q. P. Ha, "Parameterised quadratic constraints for network systems subject to multiple communication topologies," *Proc. of the 12^{th} International Conference on Control, Automation, Robotics and Vision,* ICARCV'12, pp. 221–226, Guangzhou, China 2012.

[6] Tri Tran, K.-V. Ling, and J. M. Maciejowski, "Model predictive control via quadratic dissipativity constraint," *submitted to IEEE Decision and Control Conference*, Los Angeles, CA, December 2014.

[7] Kundur, P, *Power System Stability and Control*. India: McGraw-Hill Education, 1994.

[8] Sauer, P. W. and M. A. Pai, *Power System Dynamics and Stability*. Englewood Cliffs, NJ: Prentice-Hall, 1998.

[9] Tri Tran and K.-V. Ling, "Model predictive control for nonlinear input-affine systems with stability and feasibility constraints," *submitted to IEEE Intl. Conf. Auto. Ctrl. Robotic and Vision*, Singapore, December 2014.

[10] Venkat A. N., I. A. Hisken, J. B. Rawlings, and S. J. Wright, "Distributed MPC strategies with applications to power system automatic generation control," *IEEE Trans CST*, vol. 16, pp. 1192–1206, 2008.

[11] Bhatti, T. S., A. A. F. Al-Ademi, and N. K. Bansal, "Load frequency control of isolated wind diesel hybrid power systems," *Energy Conversion and Management*, vol. 38, no. 9, pp. 829–837, 1997.

[12] Chedid, R. B., S. H. Karaki, and C. El-Chamali, "Adaptive fuzzy control for wind-diesel weak power systems," *IEEE Trans Energy Conversion*, vol. 15, no. 1, pp. 71–78, 2000.

[13] Ling, K-V., J. Maciejowski, A. Richards, and B. F. Wu, "Multiplexed model predictive control," *Automatica*, vol. 48, pp. 396–401, 2012.

[14] Angeli D., R. Amrit, and J. B. Rawlings, "On average performance and stability of economic model predictive control," *IEEE Trans AC*, vol. 57(7), pp. 1615–1626, 2012.

[15] Willems J. C., "Dissipative dynamical systems," *European Journal of Control*, vol. 13, pp. 134–151, 2007.

[16] Brogliato B., R. Lozano, B. Maschke, and O. Egeland, *Dissipative Systems Analysis and Control: Theory and Apps.* Springer, 2006.

[17] Sontag E. D. and Y. Wang, "New characterizations of input to state stability," *IEEE Trans AC*, vol. 41, no. 9, pp. 1283–1294, 1996.

[18] Kerrigan, E. C. and J. M. Maciejowski, "Invariant sets for constrained nonlinear dicrete time systems with application to feasibility in model predictive control," *Proc. of the 39^{th} IEEE CDC*, pp. 4951–4956, Sydney, Australia, 2000.

[19] Blanchini, F., "Set invariant in control," *Automatica*, vol. 35, pp. 1747–1767, 1999.

[20] Willems J. C., "Dissipative dynamical systems , Parts I and II," *Arch. Rational Mechanics Analysis*, vol. 45, pp. 321–393, 1972.

[21] Anderson, P. M. and A. A. Fouad, *Power System Control and Stability, 2^{nd} Edition*. IEEE Press - Piscataway, NJ: Wiley-Interscience, 2003.

[22] Wood A. J. and B. F. Woolenberg, *Power Generation Operation and Control, 2^{nd} Edition*. NewYork: John Wiley & Son, 1996.